ON THE INTERACTION BETWEEN SEA BREEZE AND SUMMER MISTRAL AT THE EXIT OF THE RHÔNE VALLEY DURING THE ESCOMPTE EXPERIMENT

S. Bastin[1,*], P. Drobinski[1], O. Bock[1], J.L. Caccia[2], B. Campistron[3], C. Champollion[4], A.M. Dabas[5], P. Delville[6], V. Guénard[2], F. Masson[4], O. Reitebuch[7], C. Werner[7]

[1] IPSL SA, Paris, France; [2] LSEET, Toulon, France; [3] LA, Toulouse, France ; [4] LDL, Montpellier, France ; [5] CNRM, Toulouse, France ; [6] DT INSU, Meudon, France ; [7] DLR, Wessling, Germany
[*] Current affliliation : NCAR, Boulder, CO, USA
E-mail: *bastind@ucar.edu*

Abstract: The abstract investigates experimentally and numerically the structure of a combined Mistral sea breeze event at the exit of the Rhône valley in southeastern France, as well as the near shoreline water variability at the alternation between the Mistral and the sea breeze.

Keywords – Mistral, breeze, ESCOMPTE, numerical modeling

1. INTRODUCTION

In Provence, southern France (see Fig. 1), the sea breeze shares its occurrence with the Mistral. The sea breeze advects moist air onshore and its inland penetration strongly depends on the large scale flow (Arritt, 1993). The Mistral refers to a severe northerly gap flow that develops along the Rhône valley separating the French Alps from the Massif Central. The Mistral brings cold and dry continental air over sea. In general, the Mistral is strong enough to maintain the sea breeze front offshore but during the ESCOMPTE field experiment (Cros et al., 2004), between 21 and 23 June 2001, the weak intensity of the Mistral allowed the sea breeze to break through during daytime (Guénard et al., 2005).

In the present paper, we describe the complex interaction between the sea breeze and this weak summer Mistral case which leads to very fast and short transition in time between the Mistral and the sea breeze along the coastline and show how this this complexity affects the water vapor variability. For this purpose, we use the combination of the measurements collected during the field experiment and 3-km resolution numerical simulation using the non-hydrostatic model Méso-NH (for details on the instrumental set-up and model see Bastin et al., 2005a).

Figure 1. Panel a: Map of France with the topography shaded in grey when higher than 500 m above sea level (ASL). The rectangle displays the large domain (hereafter called domain 1) of the Méso-NH simulations. Panel b: Domain 1 of the Méso-NH simulation with its nested smaller domain (hereafter called domain 2) in the rectangle. The acronyms NIM, LYO and VAL stand for the city names Nîmes, Lyon and Valence, respectively. Panel c: Domain 2 of the Méso-NH simulation. The acronyms AIX, MRS, STC and STR correspond to the city names Aix en Provence, Marseille, Saint Chamas, and Saint Rémy, respectively.
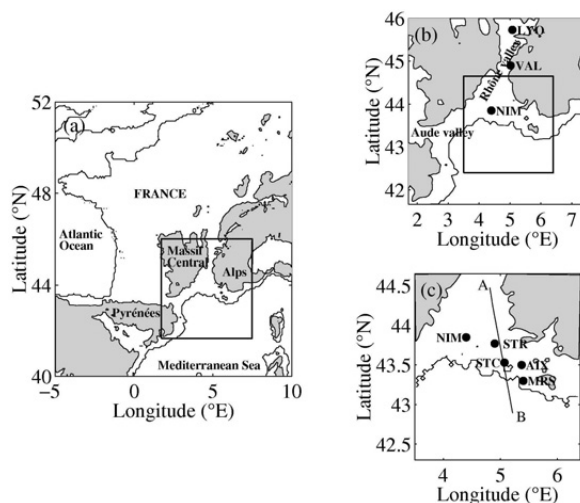
2. UNSTEADY ASPECTS OF THE 22 JUNE 2001 SEA BREEZE/MISTRAL EVENT

At 0900 UTC, the flow pattern at the exit of the Rhône valley is shown in Fig. 2 which displays the simulated and measured surface temperature and wind fields. The horizontal representation of the measured wind field is obtained by interpolating the Méso-NH fields at the locations of the Météo-France surface stations. Figure 2 shows that the Mistral blows over the nearly entire area, except for two regions: on the western side of the domain (longitude lower than 4°E) and on the eastern side of the domain (longitude greater than 5.6°E). Indeed, these are two sheltered area in the wakes trailing downstream the Massif Central and the western Alps, respectively. The Mistral brings cold and dry continental air and inhibits temperature rise. The temperature gradient between sea and land is thus damped and contributes to delay the sea breeze onset in the region where the Mistral blows. On the contrary, in the sheltered area, the temperature naturally increases with radiative heating (in the sheltered area, the temperature increases from 28°C to 30°C) and thus the sea breeze commences at a time expected in pure sea breeze events (Bastin et al., 2005b; Bastin and Drobinski, 2005a,b). The presence or absence of the Mistral blowing in some regions of the investigated target area contributes to the time and space inhomogeneity of the sea breeze, whereas in pure sea breeze events, the sea breeze onset occurs everywhere at the same time in the target area (see examples for the 25 and 26 June 2001 sea breeze events in Bastin et al., 2005b). One can also note the asymmetry of the Mistral structure in the Rhône valley. The Mistral sticks to the western Alps flank whereas it detaches from the Massif Central after the maximum constriction near Valence, when it takes a cyclonic curvature due to the Genoa cyclone (or at least to the leeside trough downstream the Alps). Méso-NH well reproduces the flow structure except for the western Alps wake located to much to the east (longitude greater than 6°E).

Figure 2. Wind and temperature fields from meteorological surface stations (left column) and Méso-NH simulations (right colum) on 22 June 2001 at 0900 (a and b), 1100 (c and d), 1400 (e and f) and 1700 UTC (g and h). The topography mask corresponds to topographical elements higher than 500 m ASL. The arrows indicate the wind direction and their scale indicate the intensity. The isolines indicate the temperature. Contour interval is 3°C from 23 to 35°C. The sea breeze front location is indicated by a thick dashed line.
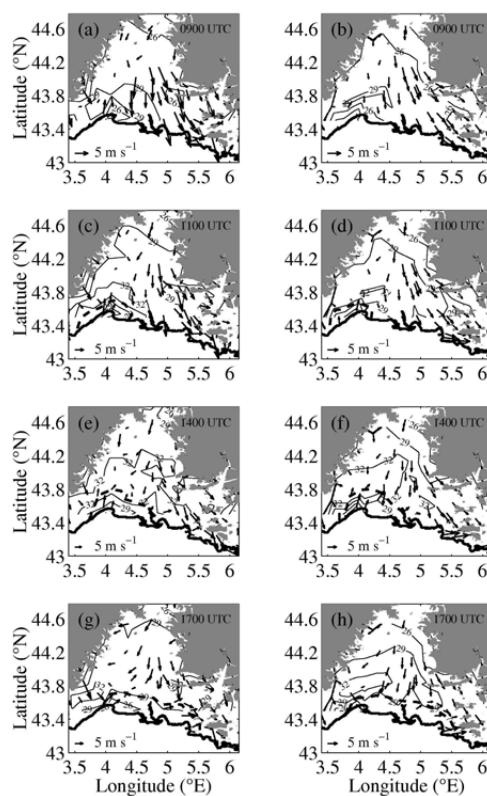
At 1100 UTC (Fig. 2), both the data and the simulation show a surface temperature gradient near the coastline on the sheltered western region of the target area (longitude 4°E) (the temperature increases from 28°C to 32°C). The sea breeze penetrates inland over a small horizontal range. The sea breeze front location is indicated by a thick dashed line. The location of the sea breeze front is determined by associating the location of the maximum of temperature and the area where the wind reverses from the south (sea breeze flow) to the north (Mistral flow). One can also notice that the northwesterly Mistral flow descends the slope of the Massif Central in its southern part whereas a wake trailing downstream the Massif Central, in the north part of the domain, is associated with very weak winds. The Mistral is bounded by the western Alps flank to the east and by the Massif Central wake to the west at about 4.5°E (Jiang et al., 2003). In the region where the Mistral blows, the sea breeze can not penetrate inland. The surface wind and temperature fields are accurately simulated with Méso-NH, despite the slight bias in temperature and the western Alps wake located too far to the east.

At 1400 UTC, the region where the sea breeze penetrates now extends further to the east. In the western side of the domain, the sea breeze front has progressed inland. The maximum penetration of the sea breeze is observed at about 43.85°N (between 3.8 and 4.3°E) versus 43.75°N for the simulation. Between 1400 and 1700 UTC, the

sea breeze front progresses inland in the center of the Rhône valley (longitude 4.5°E). The front line has "moved" eastwards and at 1700 UTC, the sea breeze does not penetrate inland in the western side of the target area, downstream the Massif Central. At 1700 UTC, the sea breeze blows in the Marseille area where it takes a westerly direction because of the coastline shape (Bastin and Drobinski, 2005a,b) and probably because it combines with the Mistral. The observations indicate a large region in the Rhône valley (between 43.7 and 44.4°N) where there is no temperature gradient and where the sea breeze and the Mistral collide (at 43.8°N). Méso-NH underestimates the spatial extension of this region and the surface temperature north of 44°N. This leads to a negative temperature gradient which prevents the sea breeze to penetrate further inland and thus explains why Méso-NH underestimates the onshore penetration of the sea breeze (the sea breeze front location is simulated at 43.8°N in the center of the Rhône valley).

Finally, the description of the flow blowing in the investigated target area allows to compare the sea breeze main features studied by Bastin et al. (2005b) for situations of sea breeze only with those for the present situation of combined sea breeze and Mistral. It shows that the cold and dry Mistral flows blowing against the sea breeze (i) delays the sea breeze onset in the region where it blows (the sea breeze breakthrough at Marseille is at 0800-1000 UTC for pure sea breeze and 1500 UTC for this case); (ii) limits the vertical and horizontal extents of the sea breeze (the sea breeze is about 1500 m deep and penetrates inland on a horizontal range of about 100 km for pure sea breeze whereas it is about 700 m deep and penetrates inland on a horizontal range of about 50 km for this case) and (iii) redirects the sea breeze (the sea breeze blows from the south south-west at Marseille for pure sea breeze and from the west for this case).

3. WATER VAPOR VARIABILITY OVER MARSEILLE

Figure 3 shows vertical profiles of water vapor density versus time from GPS tomography and from Méso-NH simulation at Marseille (MRS in Fig. 1) (see Champollion et al., 2005 for further details on GPS tomography). The simulated wind (Fig. 3b) shows that the Mistral blows from the northwest until about 1500 UTC. During that period, both GPS tomography and the simulation show a moist 800-m deep layer (about 8-9 g m^{-3} with GPS tomography and about 7-8 g m^{-3} with Méso-NH) below a dryer layer (5-6 g m^{-3}) which tops at about 2 km above ground level (AGL) at 0000 UTC. With GPS tomography, both the moist and the dryer layers tighten between 0000 and 0500 UTC. Between 0500 and 1200 UTC, the depth and the water vapor density of these two layers are nearly constant. The depth of the two layers begins to increase after 1200 UTC, but the water vapor density near the surface seems to increase at 1500 UTC. The results of Méso-NH display variations of the depth and water vapor density that are different from GPS tomography. In the morning, the variation with time of the dryer layer depth is much smoother. Between 1200 and 1500 UTC, Méso-NH shows a decrease of the water vapor density in the lowest layer by about 1.5 g m^{-3} (Fig. 3b) but is not seen in GPS tomography (Fig. 3a). During this period the layers start to deepen in the GPS measurements while the dryer layer goes on making thinner in the model results. We believe this is due to unresolved small-scale dynamics by Méso-NH run with a 3 km mesh grid. At 1500 UTC, the low-level wind veers from the northwest to the west southwest indicating the sea breeze onset over Marseille. Both GPS tomography and the simulation show a deepening and moistening of the lower levels of the troposphere. There again, we can identify two moist layers, which are more clearly visible with GPS tomography. The very moist layer (about 8-9 g m^{-3} with GPS tomography and about 9-10 g m^{-3} with Méso-NH) is about 1200-m deep. Above, a dryer layer (about 5-7 g m^{-3} with GPS tomography and about 8-9 g m^{-3} with Méso-NH) tops at about 2 km AGL between 1500 and 2400 UTC. The comparison between the water vapor field and the vertical profiles of wind speed and direction illustrates the difficulty to define the sea breeze depth. Indeed, between 1500 and 2200 UTC, the low-level wind blows from the west southwest up to about 700 m AGL. Above 700 m AGL, the wind veers to the northwest marking the presence of the Mistral. However, between 700 m and 2000 m AGL, both GPS tomography and Méso-NH show enhanced moisture marking the advection of marine air mass by the sea breeze. As suggested by Bastin and Drobinski (2005a), the sea breeze and the Mistral are not separated by a rigid lid preventing any exchanges and mixing. Most probably, a smooth transition occurs between the sea breeze and the Mistral flow aloft, which is hardly visible on the wind direction but is much clearer with the water vapor field, especially from GPS. Bastin and Drobinski (2005a) showed numerically that at the sea breeze head, mixing occurs caused by enhanced turbulence due to strong horizontal gradients of wind speed and direction and air density. At the front, air masses are lofted upward and mass can be advected from the sea breeze into the lower free troposphere. GPS tomography confirms experimentally Bastin and Drobinski (2005a) results.
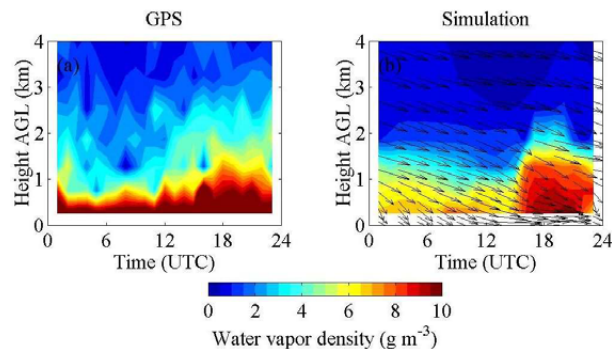
Figure 3. Time versus height plots of water vapor density over Vallon d'Ol as retrieved from the GPS tomography (a) and from Méso-NH simulation (b). The arrows indicate the horizontal wind vectors from the Méso-NH simulation.

4. CONCLUSION

We have investigated experimentally and numerically the structure of a combined Mistral sea breeze event at the exit of the Rhône valley. The sea breeze and the Mistral co-exist because of the weakness of this Mistral event. The presence of the Mistral and the various mechanisms that drive its dynamics in different regions of the Rhône valley lead to a very inhomogeneous and unsteady behavior of the sea breeze at the scale of the Rhône valley exit. The fast transition between the Mistral and the sea breeze leads to large variability of the water vapor near the shore. This variability is investigated from GPS tomography which has provided a unique data set for the description of the water vapor variability at small scale which was relevant for the analysis of a Mistral sea breeze event. This data set provided a validation for the water vapor field simulated with the Méso-NH model (see also Bastin et al., 2005c).

REFERENCES

Bastin S., Drobinski P., 2005a: Sea Breeze Induced Mass Transport over Complex Terrain in Southeastern France: A Case Study. *Quart. J. Roy. Meteorol. Soc.*, in revision

Bastin S., Drobinski P., 2005b: Temperature and Wind Velocity Oscillations along a Gentle Slope during Sea-Breeze Events. *Boundary Layer Meteorol.*, **114**, 573-594

Bastin S., Drobinski P., Guénard V., Caccia J.L., Campistron B., Dabas A. M., Delville P., Reitebuch O., Werner C., 2005a: On the Interaction Between Sea Breeze and Summer Mistral at the Exit of the Rhône Valley. *Mon. Wea. Rev.*, in revision

Bastin S., Drobinski P., Dabas A.M., Delville P., Reitebuch O., Werner C., 2005b: Impact of the Rhône and Durance Valleys on Sea-Breeze Circulation in the Marseille Area. *Atmos. Res.*, **74**, 303-328

Bastin S., Champollion C., Bock O., Drobinski P., Masson F., 2005c: On the Use of GPS Tomography to Investigate Water Vapor Variability During a Mistral Sea Breeze Event in Southeastern France. *Geophys. Res. Let*, **32**, L05808, doi:10.1029 2004GL021907

Champollion, C., F. Masson, M.N. Bouin, A. Walpersdorf, E. Doerflinger, O. Bock and J. Van Baelen, 2005: GPS Water vapour tomography: Preliminary results from the ESCOMPTE field experiment. *Atmos. Res.*, **74**, 253–274.

Cros B., Durand P., Cachier H., Drobinski P., Frejafon E., Kottmeier C., Perros P.E., Peuch V.-H., Ponche J.L., Robin D., Saïd F., Toupance G., Wortham H., 2004: The ESCOMPTE Program: An Overview. *Atmos. Res.*, **69**, 241-279

Guénard V., Drobinski P., Caccia J.L., Campistron B., Bénech B., 2005: Experimental Investigation of the Mesoscale Dynamics of the Mistral. *Boundary Layer Meteorol.*, **115**, 263-288.